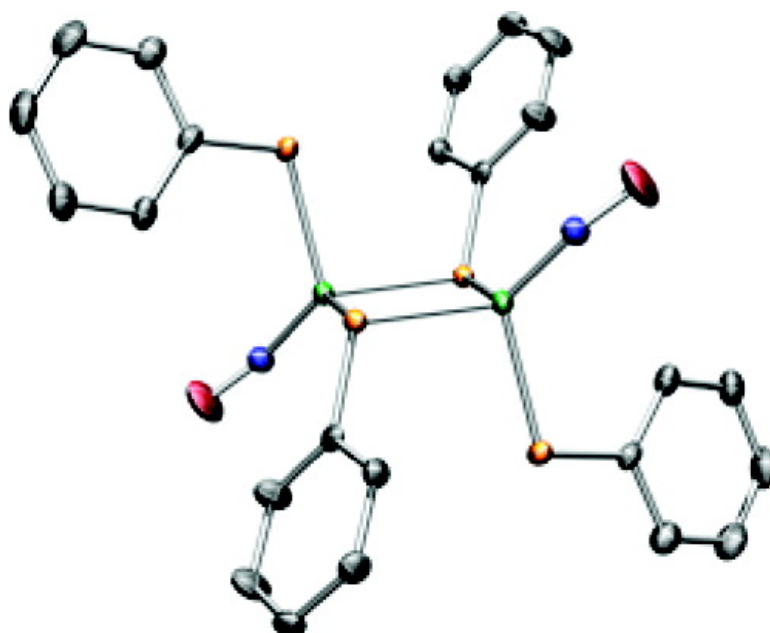


Synthesis and Characterization of {Ni(NO)} and {Co(NO)} Complexes Supported by Thiolate Ligands

Andrew G. Tennyson, Shanta Dhar, and Stephen J. Lippard

J. Am. Chem. Soc., 2008, 130 (45), 15087-15098 • DOI: 10.1021/ja803992y • Publication Date (Web): 17 October 2008

Downloaded from <http://pubs.acs.org> on February 8, 2009



More About This Article

Additional resources and features associated with this article are available within the HTML version:

- Supporting Information
- Access to high resolution figures
- Links to articles and content related to this article
- Copyright permission to reproduce figures and/or text from this article

[View the Full Text HTML](#)



ACS Publications
High quality. High impact.

Synthesis and Characterization of $\{\text{Ni}(\text{NO})\}^{10}$ and $\{\text{Co}(\text{NO})_2\}^{10}$ Complexes Supported by Thiolate Ligands

Andrew G. Tennyson, Shanta Dhar, and Stephen J. Lippard*

Department of Chemistry, Massachusetts Institute of Technology, Cambridge, Massachusetts 02139

Received May 28, 2008; E-mail: lippard@mit.edu

Abstract: Nitric oxide is an important molecule in biology and modulates a variety of physiological and pathophysiological processes. Some of its regulatory functions are exerted through interactions with redox-active elements, including iron, nickel, cobalt, and sulfur. Metalloenzymes containing $[n\text{Fe}-n\text{S}]$ ($n = 2$ or 4) clusters can be activated or inactivated by reaction with NO, affording dinitrosyl iron complexes. Studies of the NO chemistry of small-molecule iron thiolate complexes have provided insight into these biological processes and suggested probable intermediates. To explore this chemistry from a different perspective, we prepared nickel and cobalt thiolate complexes and investigated their reactions with NO and related compounds. We report here the first examples of anionic complexes containing $\{\text{Ni}(\text{NO})\}^{10}$ and $\{\text{Co}(\text{NO})_2\}^{10}$ units, the reactivity of which suggests possible intermediates in the interconversion of iron thiolate nitrosyl compounds. Our results demonstrate new chemistry involving NO and simple complexes of nickel and cobalt supported by thiolates, which have been known for more than 30 years. The use of mass balance methodology was key to their discovery. Among the novel complexes reported are $(\text{Et}_4\text{N})_2[\text{Ni}(\text{NO})(\text{SPh})_3]$ (**2**), from $(\text{Et}_4\text{N})_2[\text{Ni}(\text{SPh})_4]$ (**1**) and NO, $(\text{Et}_4\text{N})_2[\text{Ni}_2(\text{NO})_2(\mu\text{-SPh})_2(\text{SPh})_2]$ (**3**), from **1** and NO^+ or 2 and Me_3O^+ , $(\text{Et}_4\text{N})[\text{Co}(\text{NO})_2(\text{SPh})_2]$ (**5**), from $(\text{Et}_4\text{N})_2[\text{Co}(\text{SPh})_4]$ (**4**) and NO, and $[\text{Co}_3(\text{NO})_6(\mu\text{-SPh})_3]$ (**6**), from **5** and Me_3O^+ . In the syntheses of **2** and **5**, NO could be replaced by the convenient solid Ph_3CSNO .

Introduction

Nitric oxide plays important roles in biology, including signaling in the central nervous system, activation of immune response, regulation of protein function, and drug resistance.^{1–3} In many instances, these activities involve binding to a metal ion, often a heme. There are a variety of non-heme targets for NO, however, including iron–sulfur clusters. Mitochondrial aconitase, for example, houses a $[4\text{Fe}-4\text{S}]$ cluster in its active form.⁴ Reaction of the EPR-silent cluster in this enzyme with NO shuts down its activity and affords an EPR spectrum indicative of a $[3\text{Fe}-4\text{S}]$ cluster having nearly identical geometric parameters and formation of a dinitrosyl iron complex (DNIC).⁵ In another example, NO activates the transcription factor SoxR, which contains a $[2\text{Fe}-2\text{S}]$ cluster, via DNIC formation.⁶

In order to elucidate the fundamental chemistry underlying these processes, we^{7,8} and others^{9,10} have undertaken a systematic investigation of the nitric oxide chemistry of synthetic iron thiolate complexes. The conversion of homoleptic $[\text{Fe}(\text{SR})_4]^{2-}$ species by NO into DNICs proceeds through mononitrosyl iron complexes (MNICs). MNICs have not yet been unambiguously identified in protein regulation, but reactions of non-heme mononitrosyl iron complexes with NO yield EPR spectra similar to those observed for

the synthetic complexes.^{11–13} Moreover, the conversion of a $[2\text{Fe}-2\text{S}]$ cluster into DNICs could involve intermediate formation of two monometallic MNICs or a single dimetallic center containing two mononitrosyl iron units.

In contrast, homoleptic thiolate complexes of nickel and cobalt have never been observed in biology, and very little is known about their nitric oxide chemistry. The A cluster of acetyl-coenzyme A synthase/carbon monoxide dehydrogenase contains a $[4\text{Fe}-4\text{S}]$ cluster bridged by a cysteine to a three-coordinate nickel thiolate center, which is connected to a four-coordinate N_2S_2 -bound nickel species. Because iron–sulfur clusters react with NO and the natural substrate for this enzyme is CO, it is plausible that nitric oxide interacts with the enzyme in vivo at iron, nickel, or sulfur. Although lacking a cobalt(II) thiolate bond, the reduced form of cobalamin binds NO very rapidly and tightly.¹⁴ This cobalt(II) unit is essential for methionine synthesis and C_1 metabolism; treatment of cells with

- (1) Calabrese, V.; Mancuso, C.; Calvani, M.; Rizzarelli, E.; Butterfield, D. A.; Stella, A. M. *G. Nature Rev. Neurosci.* **2007**, *8*, 766–775.
- (2) Turchi, J. J. *Proc. Natl. Acad. Sci. U.S.A.* **2006**, *103*, 4337–4338.
- (3) Bronte, V.; Zanovello, P. *Nature Rev. Immunol.* **2005**, *5*, 641–654.
- (4) Robbins, A. H.; Stout, C. D. *Proc. Natl. Acad. Sci. U.S.A.* **1989**, *86*, 3639–3643.
- (5) Kennedy, M. C.; Antholine, W. E.; Beinert, H. *J. Biol. Chem.* **1997**, *272*, 20340–20347.
- (6) Ding, H.; Demple, B. *Proc. Natl. Acad. Sci. U.S.A.* **2000**, *97*, 5146–5150.

- (7) Harrop, T. C.; Song, D.; Lippard, S. J. *J. Am. Chem. Soc.* **2006**, *128*, 3528–3529.
- (8) Harrop, T. C.; Song, D.; Lippard, S. J. *J. Inorg. Biochem.* **2007**, *101*, 1730–1738.
- (9) Lu, T.-T.; Chiou, S.-J.; Chen, C.-Y.; Liaw, W.-F. *Inorg. Chem.* **2006**, *45*, 8799–8806.
- (10) Chiang, C.-Y.; Miller, M. L.; Reibenspies, J. H.; Darensbourg, M. Y. *J. Am. Chem. Soc.* **2004**, *126*, 10867–10874.
- (11) Chen, V. J.; Orville, A. M.; Harpel, M. R.; Frolik, C. A.; Surerus, K. K.; Münck, E.; Lipscomb, J. D. *J. Biol. Chem.* **1989**, *264*, 21677–21681.
- (12) Arciero, D. M.; Lipscomb, J. D.; Huynh, B. H.; Kent, T. A.; Münck, E. *J. Biol. Chem.* **1983**, *258*, 14981–14991.
- (13) Rich, P. R.; Salerno, J. C.; Leigh, J. S.; Bonner, W. D., Jr. *FEBS Lett.* **1978**, *93*, 323–326.
- (14) Wolak, M.; Zahl, A.; Schnepfensieper, T.; Stochel, G.; van Eldik, R. *J. Am. Chem. Soc.* **2001**, *123*, 9780–9791.

NO donors disrupts these functions,¹⁵ suggesting a role for NO in regulating C₁ metabolism.

Previous reactivity studies of simple iron thiolate complexes with NO suggest that intermediates exist in the formation of multimetallic iron nitrosyl species that have not yet been observed. Low-temperature in situ spectroscopy might reveal their existence but would not yield as much information as isolation and characterization of discrete complexes. An alternative is to study the nitric oxide chemistry of analogous thiolate complexes of the adjacent transition metals cobalt and nickel. Electronic configurations or geometries that are transient or unstable for iron may be more robust when these other metals are employed. Furthermore, by studying the reactivity of simple thiolate complexes of nickel and cobalt with NO, we might gain insight into how nitric oxide could interact with complexes of these metals in vivo and guide potential future enzymatic investigations. We therefore extended our studies to include reactions of nickel(II) and cobalt(II) thiolate complexes with NO(g), NOBF₄, and Ph₃CSNO, beginning with the homoleptic [M(SPh)₄]²⁻ ions. Despite the simplicity of this system and the availability of the reactants for more than a decade, their chemistry remained unexplored. Herein we report the first results of our investigation.

Experimental Section

Materials and Methods. Metal salts and porphyrinato complexes were purchased from Strem Chemicals and organic reagents from Aldrich Chemical Co. or Alfa Aesar and used as received. Solvents were dried and purified by passage through alumina columns under an argon atmosphere. (Et₄N)₂[Ni(SPh)₄] (**1**) and (Et₄N)₂[Co(SPh)₄] (**4**) were prepared by literature methods.^{16,17} Ph₃CSNO was prepared by a modification of an established procedure.¹⁸ Air- and water-sensitive manipulations were carried out under a dry nitrogen or argon atmosphere using standard Schlenk or glovebox techniques. Nitric oxide gas was purified following a reported procedure¹⁹ by passage first through a 2 m stainless steel coil packed with silica and cooled to -78 °C, then through an Ascarite column. Manipulations and transfers of purified NO(g) were performed with gas-tight syringes under an inert atmosphere.

General Spectroscopic Considerations. NMR spectra were recorded at 22 °C on a 400 MHz Bruker Avance spectrometer. Chemical shifts for ¹H and ¹³C NMR spectra are expressed in ppm relative to residual solvent (CD₂HCN in CD₃CN, 1.94 and 1.24 ppm for ¹H and ¹³C, respectively). FT-IR spectra were recorded on a Thermo Nicolet Avatar 360 spectrophotometer running the OMNIC software. Solid samples were examined as KBr discs. Solution FT-IR spectra were acquired in a gas-tight Graseby-Specac solution cell equipped with CaF₂ windows and 0.1 mm Teflon spacers. UV-visible absorption spectra were recorded on a Cary 50 spectrophotometer at 25 °C. Stirring and temperature control were performed with a Quantum Northwest TC125 Peltier device. All measurements were made with a matched pair (blank and sample) of 6Q Spectrosil quartz cuvettes (Starna) with 1 cm path lengths and 3.0 mL sample solution volumes. The sample cuvette was sealed with a gas-tight Teflon-lined screw cap equipped with a septum.

X-ray Crystallographic Studies. Single crystals were mounted at room temperature within microfiber loops immersed in Paratone-N oil and cooled to 110 K under a stream of cold nitrogen. Intensity data were collected on a Bruker APEX CCD diffractometer running the SMART software package, with Mo K α radiation (λ = 0.71073 Å). The structures were solved by direct methods and refined by using the SHELXTL^{20,21} software package. Empirical absorption corrections were applied with SADABS,²² part of the SHELXTL program package, and the structures were checked for higher symmetry by the program PLATON.²³ All non-hydrogen atoms were refined anisotropically. Hydrogen atoms were placed at calculated positions and assigned thermal parameters equal to either 1.5 (methyl hydrogen atoms) or 1.2 (non-methyl hydrogen atoms) times the thermal parameters of the atoms to which they were attached. Complex **3** crystallizes with one CH₃CN molecule in the asymmetric unit, and the nitrogen atom was refined in two positions, each with half-occupancy. Parameters for **2**, **3**, **5**, and **6** are listed in the Supporting Information (Tables S1–S4).

General Procedure for Mass Balance Analyses. Reactions were quenched by addition to 10 volume equiv of Et₂O and cooled to -30 °C for 2 h, after which the precipitate and supernatant were separated by filtration. The filtrate was transferred to a Schlenk flask, cycled out of the drybox, and stripped on a vacuum line without heating (room-temperature water bath). The residue from the filtrate was washed three times with 3 mL of solvents with increasing polarity, Et₂O < THF < CH₃CN, to extract separately the components present. Each wash was filtered into a separate tared vial, the solvent removed, and the mass recorded. GC-MS was performed on the white solid isolated from the Et₂O fraction and the result compared with that of authentic Ph₂S₂. When Ph₃CSNO rather than NO was used as the NO-donating reagent, a statistical mixture of Ph₂S₂, PhSSCPh₃, and Ph₃CSSCPh₃ was observed. To calculate the percent yield of disulfide in this case, the average molecular weight was computed from the relative contribution of each disulfide to the total mixture; e.g., for a 1:2:1 mixture, 0.25(Ph₂S₂) + 0.5(PhSSCPh₃) + 0.25(Ph₃CSSCPh₃) = 0.25(218.34) + 0.5(384.56) + 0.25(550.77) = 384.56 g mol⁻¹. The THF and CH₃CN extracts from the filtrate residue and precipitate were analyzed separately by IR and ¹H NMR spectroscopy and combined only after their identities were confirmed.

Syntheses. (Et₄N)₂[Ni(NO)(SPh)₃] (2**).** From **1** + NO(g). In 5 mL of CH₃CN was dissolved 75.1 mg of **1** (99.4 μ mol), and into the resulting dark red solution was bubbled 2.5 mL of NO(g) (102 μ mol), affording a gradual color change to blue-green. This solution was allowed to stir for 30 min at room temperature and was then added to 100 mL of Et₂O, causing the formation of a white-green suspension. After this mixture was cooled to -30 °C for 2 h, a blue-green microcrystalline product had formed along with a light green supernatant. The precipitate was collected by filtration, and the filtrate was stripped to afford a mixture of white and blue-green solids. Mass balance analysis was performed, and from this reaction were isolated 9.0 mg of Ph₂S₂ (41 μ mol, 82%) and 65 mg of **2** (96 μ mol, 97%).

From **1 + Ph₃CSNO.** In 5 mL of CH₃CN was dissolved 77.8 mg of **1** (103 μ mol), and to the resulting dark red solution was added 32.4 mg of Ph₃CSNO (106 μ mol) in 5 mL of CH₃CN, affording a gradual color change to blue-green. This solution was allowed to stir for 30 min at room temperature and was then added to 100 mL of Et₂O, causing the formation of a white-green suspension. After this mixture was cooled to -30 °C for 2 h, a blue-green microcrystalline product had formed along with a light green supernatant. The precipitate was collected by filtration, and

(15) Danishpajooh, I. O.; Gudi, T.; Chen, Y.; Kharitonov, V. G.; Sharma, V. S.; Boss, G. R. *J. Biol. Chem.* **2001**, *276*, 27296–27303.

(16) Yamamura, T.; Miyamae, H.; Katayama, Y.; Sasaki, Y. *Chem. Lett.* **1985**, 269–272.

(17) Dance, I. G. *J. Am. Chem. Soc.* **1979**, *101*, 6264–6273.

(18) (a) Josephy, P. D.; Rehorek, D.; Janzen, E. G. *Tetrahedron Lett.* **1984**, *25*, 1685–1688. (b) Arulsamy, N.; Bohle, D. S.; Butt, J. A.; Irvine, G. J.; Jordan, P. A.; Sagan, E. *J. Am. Chem. Soc.* **1999**, *121*, 7115–7123. (c) Harrop, T. C.; Tonzetich, Z. J.; Reisner, E.; Lippard, S. J. *J. Am. Chem. Soc.* **2008**, *130*, in press (<http://dx.doi.org/ja8054996>).

(19) Tran, D.; Skelton, B. W.; White, A. H.; Laverman, L. E.; Ford, P. C. *Inorg. Chem.* **1998**, *37*, 2505–2511.

(20) Sheldrick, G. M. *SHELXTL*; University of Göttingen: Göttingen, Germany, 2000.

(21) Sheldrick, G. M. *SHELXTL*, v 6.10; Bruker AXS: Madison, WI, 2001.

(22) Sheldrick, G. M. *SADABS*; University of Göttingen: Göttingen, Germany, 2001.

(23) Spek, A. L. *PLATON*; Utrecht University: Utrecht, The Netherlands, 2000.

the filtrate was stripped to afford a mixture of white and blue-green solids. Mass balance analysis was performed, and from this reaction were isolated 37 mg of disulfide (96 μmol, 93%) and 66 mg of **2** (98 μmol, 95%).

Characterization of 2. ¹H NMR (CD₃CN): δ 7.62 (d, *o*-C₆H₅, 6H); 6.99 (t, *m*-C₆H₅, 6H); 6.79 (s, *p*-C₆H₅, 3H); 3.15 (q, NCH₂CH₃, 16H); 1.20 (tt, NCH₂CH₃, 24H) ppm. ¹³C NMR (CD₃CN): δ 133.7, 128.1, 120.9, 120.8, 52.9 (t, NCH₂CH₃), 7.59 (NCH₂CH₃) ppm. FT-IR (KBr): 1655 (vs, ν_{NO}), 1570 (vs), 1481 (s), 1468 (vs), 1450 (s), 1437 (m), 1390 (s), 1365 (w), 1336 (w), 1304 (w), 1261 (w), 1182 (w), 1173 (m), 1151 (w), 1126 (w), 1082 (s), 1063 (m), 1024 (m), 1003 (m), 993 (m), 964 (w), 904 (vw), 885 (w), 839 (vw), 783 (m), 739 (vs), 694 (vs), 617 (vw), 548 (w), 482 (m), 428 (w) cm⁻¹. FT-IR (CH₃CN, CaF₂): ν_{NO} = 1756 (vs) cm⁻¹. UV-vis in CH₃CN, λ (ε) in nm (M⁻¹ cm⁻¹): 372 (6260), 423 (sh, 2930), 812 (1380). Anal. Calcd for C₃₄H₅₅N₃O₃Ni: C, 60.35; H, 8.19; N, 6.21. Found: C, 59.54; H, 8.13; N, 6.09. Blue-green plates (0.14 × 0.09 × 0.04 mm) suitable for X-ray diffraction were grown by cooling a saturated solution of **2** in CH₃CN from room temperature to -30 °C over 2 weeks.

(Et₄N)₂[Ni₂(NO)₂(μ-SPh)₂(SPh)₂] (3). **From 1 + NOBF₄.** In 5 mL of CH₃CN was dissolved 156 mg of **1** (206 μmol), and to the resulting dark red solution was added 23.1 mg of NOBF₄ (198 μmol) in 5 mL of CH₃CN, affording a gradual color change to dark brown-green. This solution was allowed to stir for 30 min at room temperature and was then added to 100 mL of Et₂O, causing the formation of a white-brown suspension. After this mixture was cooled to -30 °C for 2 h, a dark brown microcrystalline product had formed along with a dark green supernatant. Mass balance analysis was performed, and from this reaction were isolated 41 mg of Ph₂S₂ (188 μmol, 95%), 40 mg of Et₄NBF₄ (184 μmol, 93%), and 86 mg of **3** (98 μmol, 99%).

From 2 + Me₃OBF₄. In 5 mL of CH₃CN was dissolved 67.7 mg of **2** (100 μmol), and to the resulting dark blue-green solution was added 14.7 mg of Me₃OBF₄ (99.4 μmol) in 3 mL of CH₃CN, affording a gradual color change to dark green. This solution was allowed to stir for 30 min at room temperature and was then added to 100 mL of Et₂O, causing the formation of a white-green suspension. After this mixture was cooled to -30 °C for 2 h, a white solid had formed along with a dark green supernatant. Mass balance analysis was performed, and from this reaction were isolated 21 mg of Et₄NBF₄ (97 μmol, 98%) and 43 mg of **3** (49 μmol, 98%).

Characterization of 3. ¹H NMR (CD₃CN): δ 7.83 (br, *o*-C₆H₅, 8H); 7.13 (br, *m*-C₆H₅, 8H); 6.98 (br, *p*-C₆H₅, 4H); 3.12 (q, NCH₂CH₃, 16H); 1.17 (tt, NCH₂CH₃, 24H) ppm. ¹³C NMR (CD₃CN): δ 134.1, 137.8, 128.5, 123.1, 53.0 (t, NCH₂CH₃), 7.62 (NCH₂CH₃) ppm. FT-IR (KBr): 1709 (vs, ν_{NO}), 1574 (s), 1471 (s), 1433 (m), 1392 (m), 1367 (w), 1338 (vw), 1302 (w), 1265 (w), 1182 (w), 1171 (m), 1082 (s), 1065 (m), 1055 (m), 1024 (m), 1001 (m), 976 (w), 895 (w), 854 (w), 789 (m), 742 (vs), 694 (vs), 671 (vw), 615 (vw), 569 (w), 482 (m), 426 (w). FT-IR (THF, CaF₂): ν_{NO} = 1751 (vs), 1721 (vs) cm⁻¹. UV-vis in CH₃CN, λ (ε) in nm (M⁻¹ cm⁻¹): 365 (7990), 431 (sh, 3360), 639 (sh, 989), 808 (1650). Anal. Calcd for C₄₁H_{61.5}N_{4.5}O₂S₄Ni₂: C, 55.01; H, 6.93; N, 7.04. Found: C, 54.64; H, 6.60; N, 7.34. Dark green blocks (0.20 × 0.20 × 0.05 mm) suitable for X-ray diffraction were grown by vapor diffusion of Et₂O into a solution of **3** in CH₃CN at -30 °C over 3 days.

(Et₄N)[Co(NO)₂(SPh)₂] (5). **From 4 + NO(g).** In 5 mL of CH₃CN was dissolved 75.6 mg of **4** (100 μmol), and into the resulting dark green solution was bubbled 10.0 mL of NO (406 μmol), affording a gradual color change to dark brown. This solution was allowed to stir for 30 min at room temperature and was then added to 100 mL of Et₂O, causing the formation of a white-brown suspension. After this mixture was cooled to -30 °C for 2 h, a dark brown microcrystalline product had formed along with a white precipitate and a dark brown supernatant. The solids were collected by filtration, and the filtrate was stripped to afford a mixture of white and dark brown solids. Mass balance analysis was performed,

and from this reaction were isolated 10 mg of disulfide (46 μmol, 92%), 24 mg of Et₄NPh (100 μmol, 100%), and 41 mg of **5** (88 μmol, 88%).

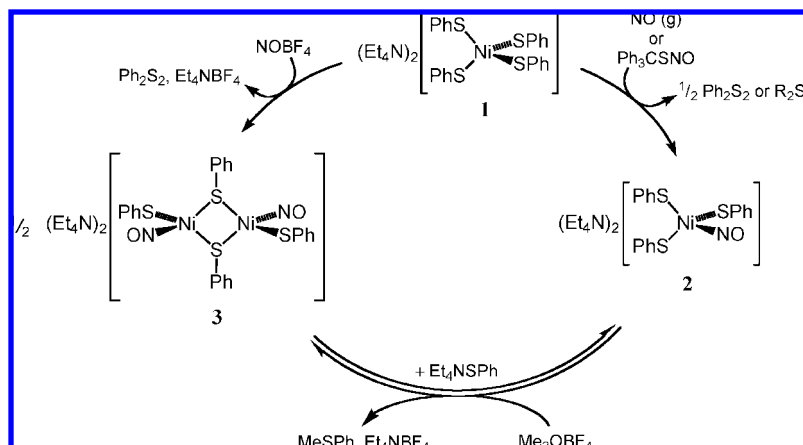
From 4 + Ph₃CSNO. In 5 mL of CH₃CN was dissolved 76.1 mg of **4** (101 μmol), and to the resulting dark green solution was added 62.0 mg of Ph₃CSNO (204 μmol) in 5 mL of CH₃CN, affording a gradual color change to dark brown. This solution was allowed to stir for 30 min at room temperature and was then added to 100 mL of Et₂O, causing the formation of a white-brown suspension. While this mixture was being cooled to -30 °C for 2 h, we observed formation of a dark brown microcrystalline product along with a dark brown supernatant. The precipitate was collected by filtration, and the filtrate was stripped to afford a mixture of white and dark brown solids. Mass balance analysis was performed, and from this reaction were isolated 56 mg of disulfide (85 μmol, 84%), 19 mg of Et₄NPh (79 μmol, 77%), and 44 mg of **5** (93 μmol, 92%).

From 4 + NOBF₄. In 5 mL of CH₃CN was dissolved 76.8 mg of **4** (102 μmol), and to the resulting dark green solution was added 11.8 mg of NOBF₄ (101 μmol) in 5 mL of CH₃CN, affording a color change to dark brown with a purple colloid. This mixture was allowed to stir for 30 min at room temperature and was then added to 100 mL of Et₂O, causing the formation of a white-brown suspension. After this mixture was cooled to -30 °C for 2 h, a dark brown microcrystalline product had formed along with a dark brown supernatant. Mass balance analysis was performed, and from this reaction were isolated 11 mg of Ph₂S₂ (50 μmol, 100%), 22 mg of Et₄NBF₄ (101 μmol, 100%), 21 mg of **5** (45 μmol, 90%), and an intractable dark purple solid.

Characterization of 5. ¹H NMR (CD₃CN): δ 7.30 (dd, *o*-C₆H₅, 4H); 7.00 (tt, *m*-C₆H₅, 4H); 6.84 (tt, *p*-C₆H₅, 2H); 3.14 (br q, NCH₂CH₃, 8H); 1.18 (br t, NCH₂CH₃, 12H) ppm. ¹³C NMR (CD₃CN): δ 148.9, 133.2, 128.3, 122.5, 53.0 (t, NCH₂CH₃), 7.68 (NCH₂CH₃) ppm. FT-IR (KBr): 1756 (vs, ν_{NO}), 1678 (vs, ν_{NO}), 1573 (s), 1558 (m), 1479 (s), 1473 (s), 1460 (s), 1433 (s), 1390 (s), 1374 (w), 1366 (m), 1335 (w), 1311 (w), 1295 (w), 1265 (w), 1170 (s), 1083 (s), 1067 (m), 1056 (m), 1020 (m), 998 (m), 895 (w), 844 (w), 781 (m), 753 (s), 749 (s), 696 (s), 480 (w), 421 (w) cm⁻¹. FT-IR (THF, CaF₂): ν_{NO} = 1769 (vs), 1699 (vs) cm⁻¹. UV-vis in CH₃CN, λ (ε) in nm (M⁻¹ cm⁻¹): 346 (sh, 6060). Anal. Calcd for C₂₀H₃₀N₃O₂S₂Co: C, 51.38; H, 6.47; N, 8.99. Found: C, 51.65; H, 6.58; N, 8.79. Dark brown-black needles (0.25 × 0.08 × 0.03 mm) suitable for X-ray diffraction were grown by vapor diffusion of Et₂O into a solution of **5** in THF at -30 °C overnight.

[Co₃(NO)₆(μ-SPh)₃] (6). In 5 mL of CH₃CN was dissolved 70.0 mg of **5** (150 μmol), and to the resulting dark brown solution was added 22.7 mg of Me₃OBF₄ (153 μmol) in 3 mL of CH₃CN, affording a gradual color change to dark red-orange. This solution was allowed to stir for 30 min at room temperature and was then added to 100 mL of Et₂O, causing the formation of cloudy red-orange solution. After this mixture was cooled to -30 °C for 2 h, a light gray precipitate had formed along with a red-orange supernatant. Mass balance analysis was performed, and from this reaction were isolated 32 mg of Et₄NBF₄ (147 μmol, 98%) and 33 mg of **6** (48 μmol, 96%).

Characterization of 6. ¹H NMR (CD₃CN): δ 7.53 (d, *o*-C₆H₅, 6H); 7.28 (t, *m*-C₆H₅, 6H); 7.19 (t, *p*-C₆H₅, 3H) ppm. ¹³C NMR (CD₃CN): δ = 134.4, 130.5, 128.3 ppm. FT-IR (KBr): 1840 (s, ν_{NO}), 1817 (s, ν_{NO}), 1779 (s, ν_{NO}), 1744 (s, ν_{NO}), 1575 (vw), 1473 (w), 1435 (vw), 1385 (vw), 1295 (vw), 1261 (w), 1152 (vw), 1011 (vw), 1080 (vw), 1066 (w), 1021 (w), 999 (vw), 800 (w), 740 (vs), 687 (s), 479 (m) cm⁻¹. FT-IR (THF, CaF₂): ν_{NO} = 1844 (m sh), 1819 (vs), 1780 (vs), 1764 (s sh) cm⁻¹. UV-vis in CH₃CN, λ (ε) in nm (M⁻¹ cm⁻¹): 325 (sh, 12 500), 421 (br sh, 6670), 656 (sh, 757). Anal. Calcd for C₁₈H₁₅N₆O₆S₃Co₃: C, 31.59; H, 2.21; N, 12.28. Found: C, 31.28; H, 2.25; N, 12.20. Dark brown-red plates (0.20 × 0.20 × 0.02 mm) suitable for X-ray diffraction were grown by cooling a saturated solution of **6** in Et₂O at room temperature to -30 °C for 1 week.

Scheme 1. Syntheses of **2** and **3**

NO Transfer Reactions. UV–Vis Spectroscopic Parameters. Using the Cary 50 scanning kinetics software, the scan window range was set to 800–200 nm, with 50 ms averaging time, 1.00 nm resolution, and 1200 nm/min scan rate; scans were acquired every 60 s for 2 h. The first scan in each experiment measured the metalloporphyrin alone. An aliquot of metal nitrosyl was added, and the solution was vigorously shaken for 3 s and then allowed to stand for an additional 7 s before beginning the second scan. Thus, a total of 10 s elapsed between injection of the metal nitrosyl and the beginning of the second scan.

Metal Nitrosyl Reactions with [Fe(TPP)Cl]. A 762 μM stock solution of [Fe(TPP)Cl] in THF was prepared, from which a 7.62 μM working solution in THF was obtained. A 2.3 mM stock solution of metal nitrosyl (**2** in CH_3CN , **3** or **5** in THF) was prepared. After a blank was acquired in THF, the spectrum of a 3 mL aliquot of the working solution of [Fe(TPP)Cl] was obtained to verify the concentration by measuring the absorption of the Soret band ($\lambda = 417$ nm, $\epsilon = 1.11 \times 10^5 \text{ M}^{-1} \text{ cm}^{-1}$). Simple NO coordination would afford [Fe(TPP)(NO)Cl], a process that does not significantly alter the UV–vis spectrum in the 400–1000 nm region.²⁴ A reductive nitrosylation reaction would afford [Fe(TPP)(NO)] with a concomitant hypsochromic shift in the Soret band ($\lambda = 405$ nm, $\epsilon = 1.00 \times 10^5 \text{ M}^{-1} \text{ cm}^{-1}$).²⁵

Reaction of **2 with [Fe(TPP)Cl].** In 5 mL of THF was dissolved 70.9 mg of [Fe(TPP)Cl] (101 μmol), and to the resulting dark red solution was added 67.1 mg of **2** (99.2 μmol) in 3 mL of CH_3CN , affording no perceptible color change. This solution was allowed to stir for 30 min at room temperature and was then added to 100 mL of Et_2O , causing the formation of a red-brown solution. After this mixture was cooled to -30 $^\circ\text{C}$ for 2 h, a sticky dark green precipitate had formed along with a red-brown supernatant. No Ph_2S_2 was isolated from the supernatant, and the IR spectrum of the dark green precipitate was identical to that of authentic **3**, with an NO stretch at 1709 cm^{-1} . Mass balance analysis could not be performed because of the similar solubilities of **3** and the porphyrin-containing product.

NO Transfer to [Co(TPP)]. A 2.01 mM stock solution of [Co(TPP)] in THF was prepared, from which a 5.03 μM working solution in THF was obtained. A 2.0 mM stock solution of **2** in CH_3CN was prepared. After a blank was acquired in THF, the spectrum of a 3 mL aliquot of the working solution of [Co(TPP)] was obtained to verify the concentration by measuring the absorption of the Soret band ($\lambda = 409$ nm, $\epsilon = 2.05 \times 10^5 \text{ M}^{-1} \text{ cm}^{-1}$).²⁶ Simple NO coordination would afford [Co(TPP)(NO)] with a

Table 1. ^1H NMR Chemical Shifts for PhS^- Ligands and Ratio of $\text{Et}_4\text{N}^+:\text{PhS}^-$ Integrals for **1–6**

	ortho	meta	para	$\text{Et}_4\text{N}^+:\text{PhS}^-$
1	1.91	21.7	−12.5	1:2
2	7.62	6.99	6.79	2:3
3	7.83	7.13	6.98	1:2 ^a
4	17.3	−24.5	−33.0	1:2
5	7.30	7.00	6.84	1:2
6	7.54	7.28	7.19	—

^a Terminal and bridging PhS^- ligands are in rapid exchange (see text and Figure S1, Supporting Information).

concomitant bathochromic shift in the Soret band and increase in absorptivity ($\lambda = 411$ nm, $\epsilon = 1.77 \times 10^6 \text{ M}^{-1} \text{ cm}^{-1}$).²⁷ In comparison, the Soret band for cobalt-reconstituted guanylyl cyclase [Co(sGC)] ($\lambda = 401$ nm, $\epsilon = 1.14 \times 10^5 \text{ M}^{-1} \text{ cm}^{-1}$) shifts hypsochromically with a decrease in absorptivity upon binding NO ($\lambda = 390$ nm, $\epsilon = 1.07 \times 10^5 \text{ M}^{-1} \text{ cm}^{-1}$).²⁸

Results and Discussion

Synthesis and Properties of the First Mononuclear $\{\text{Ni}(\text{NO})\}^{10}$ Anion (2**).** Addition of a stoichiometric amount of Ph_3CSNO to a solution of **1** in CH_3CN caused an immediate color change from dark red to dark blue-green. Mass balance analysis indicated that 1 equiv of disulfide and 1 equiv of $(\text{Et}_4\text{N})_2[\text{Ni}(\text{NO})(\text{SPh})_3]$ (**2**) were produced per equiv of **1** consumed (Scheme 1). Compound **2** is diamagnetic, and ^1H NMR spectroscopy reveals a 2:3 ratio of $\text{Et}_4\text{N}^+:$ PhS^- protons (Table 1). The NO stretch for **2** occurs at 1655 cm^{-1} in the solid state (KBr) but shifts to 1756 cm^{-1} in solution (CH_3CN). Monometallic $\{\text{Ni}(\text{NO})\}^{10}$ complexes can exhibit solvent-dependent variations in ν_{NO} by up to 50 cm^{-1} from the value measured in the solid state.²⁹ This behavior is believed to be a result of a Lewis acid–base interaction between the nitrosyl and solvent,³⁰ but the limited solubility of **2** precludes a study of ν_{NO} dependence on solvent acceptor number. Dissolving **2** in CH_3CN , removing the solvent in vacuo, and acquiring the IR spectrum in a KBr pellet or Nujol mull reveals the same

(24) Wayland, B. B.; Olson, L. W. *J. Am. Chem. Soc.* **1974**, *96*, 6037–6041.

(25) Scheidt, W. R.; Frisse, M. E. *J. Am. Chem. Soc.* **1975**, *97*, 17–21.

(26) Cruz, F. D.; Driaf, K.; Berthier, C.; Lameille, J.-M.; Armand, F. *Thin Solid Films* **1999**, *349*, 155–161.

(27) Richter-Addo, G. B.; Hodge, S. J.; Yi, G.-B.; Khan, M. A.; Ma, T.; Van Caemelbecke, E.; Guo, N.; Kadish, K. M. *Inorg. Chem.* **1996**, *35*, 6530–6538.

(28) Dierks, E. A.; Hu, S.; Vogel, K. M.; Yu, A. E.; Spiro, T. G.; Burstyn, J. N. *J. Am. Chem. Soc.* **1997**, *119*, 7316–7323.

(29) Darensbourg, D. J.; Decuir, T. J.; Stafford, N. W.; Robertson, J. B.; Draper, J. D.; Reibenspies, J. H.; Kathó, A.; Joó, F. *Inorg. Chem.* **1997**, *36*, 4218–4226.

(30) Hunter, A. D.; Legzdins, P. *Organometallics* **1986**, *5*, 1001–1009.

ν_{NO} band at 1655 cm⁻¹. According to the Enemark–Feltham convention,³¹ **2** has a {Ni(NO)}¹⁰ core, and complexes of this type are well-known. Other four-coordinate, monometallic {Ni(NO)}¹⁰ complexes are diamagnetic and display a range of NO stretching frequencies from 1558 to 1867 cm⁻¹ (avg = 1742 ± 68 cm⁻¹).^{29,32–43} Possibly, the solid-state ν_{NO} value is significantly below average because the {Ni(NO)}¹⁰ core is supported by three thiolates in a dianionic molecule, whereas the other complexes are cationic or charge neutral. Complex **2** contains the first reported example of a {Ni(NO)}¹⁰ species contained within an anionic molecule.

A preliminary reactivity study of **1** with *S*-nitroso-*N*-acetylpenicillamine (SNAP) also afforded **2**, judging by FT-IR spectroscopy, but the insolubility of SNAP in CH₃CN prevented reaction homogeneity and accurate mass balance analysis. *S*-Nitrosothiols (RSNOs), like SNAP, are prevalent in biology and believed by some to be the predominant carriers of NO. Nevertheless, the mechanism by which an RSNO delivers NO is controversial.^{44–49} The two limiting cases are RSNO delivery of NO, termed nitrosylation, and delivery of NO⁺, termed nitrosation.⁵⁰ To determine whether the RSNO species were behaving as NO or NO⁺ donors, we compared the reactivity of Ph₃CSNO and SNAP with that of NO(g). Addition of stoichiometric NO(g) to **1** afforded slow conversion to 0.5 equiv of Ph₂S₂ and 1 equiv of **2** (Scheme 1). Because the reaction of **1** with either Ph₃CSNO or SNAP yielded **2**, we conclude that these *S*-nitrosothiols are functioning as NO donors, and such behavior has been observed previously by us⁸ and others.⁹ Slow vapor diffusion of Et₂O into a solution of **2** in CH₃CN at -30 °C over 2 weeks afforded crystals suitable for X-ray diffraction, which confirmed the structural assignment of **2** (Figure 1). The average nickel nitrosyl structural parameters for **2** (Ni–N–O = 156.6°, N–O = 1.171 Å, Ni–N = 1.663 Å, Table 2s) fall within the range of reported values for other four-coordinate, monometallic {Ni(NO)}¹⁰ complexes (Ni–N–O = 149.1–180.0°,

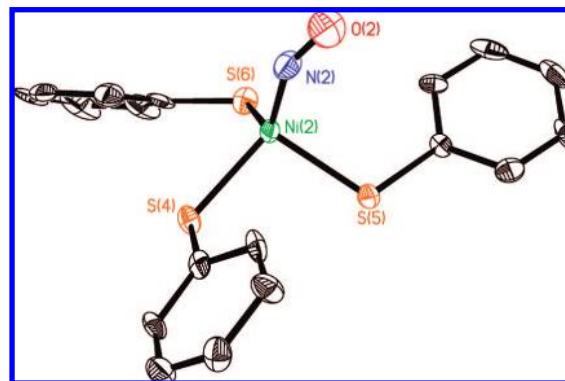


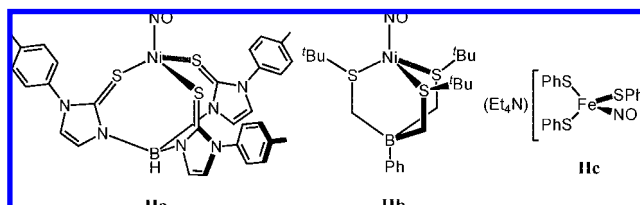
Figure 1. ORTEP diagram showing 50% probability thermal ellipsoids and selected atom labels for one of the two crystallographically distinct molecules of **2** in the crystal lattice. The Et₄N⁺ cations and H atoms are omitted for clarity. Selected bond distances (Å) and angles (deg): Ni1–O1, 1.178(9); Ni1–N1, 1.651(7); Ni1–S1, 2.339(2); Ni1–S2, 2.307(2); Ni1–S3, 2.279(2); Ni1–N1–O1, 159.0(6); S1–Ni1–N1, 121.6(2); S2–Ni1–N1, 119.9(2); S3–Ni1–N1, 105.5(2); S1–Ni1–S2, 99.67(7); S1–Ni1–S3, 106.82(7); S2–Ni1–S3, 101.14(7); N2–O2, 1.164(8); Ni2–N2, 1.674(7); Ni2–S4, 2.295(2); Ni2–S5, 2.270(2); Ni2–S6, 2.317(2); Ni2–N2–O2, 154.2(6); S4–Ni2–N2, 126.0(2); S5–Ni2–N2, 103.0(2); S6–Ni2–N2, 118.2(2); S4–Ni2–S5, 98.71(8); S4–Ni2–S6, 99.19(8); S5–Ni2–S6, 109.80(8).

Table 2. List of Bond Lengths (Å), Angles (deg), and ν_{NO} (cm⁻¹) Values for **2** and **Ila–c**

	2 ^a	Ila	Ilb	Ilc
N–O	1.171(10)	1.131(4)	1.173(2)	1.169(6)
M–N	1.663(16)	1.665(3)	1.683(2)	1.682(5)
M–S	2.328(16)	2.3503(11)	2.2915(5)	2.2780(13)
	2.301(8)	2.3432(11)	2.2838(5)	2.2696(12)
	2.275(6)	2.3190(10)	2.2775(5)	2.2670(14)
M–N–O	156.6(34)	173.9(4)	167.0(2)	164.6(5)
S–M–N	123.8(31)	121.34(11)	130.48(7)	116.52(16)
	119.1(12)	114.47(10)	117.99(6)	109.19(18)
	104.3(18)	114.01(11)	117.48(8)	108.69(18)
S–M–S	108.3(21)	103.87(4)	95.67(2)	109.47(5)
	100.2(14)	101.34(4)	94.54(2)	108.35(5)
	99.19(7)	99.30(4)	92.99(2)	103.87(5)
ν_{NO} (solid)	1655	—	1785	—
ν_{NO} (soln)	1756	1752	—	1732

^a Structural parameters are averaged from the two crystallographically distinct molecules. Numbers in parentheses represent standard deviation from mean, not ESD values.

Chart 1



avg = 165.8 ± 11.1°; N–O = 1.120–1.185 Å, avg = 1.160 ± 0.017 Å; Ni–N = 1.581–1.692 Å, avg = 1.645 ± 0.032 Å).^{29,32–43} Because the mean Ni–N–O angle for **2** is more acute than average and the N–O and Ni–N distances are longer, we conclude that the nickel atom in **2** provides greater π -backbonding to the nitrosyl. This result is consistent with the anionic environment and ligand donation ability in the nickel nitrosyl fragment of **2**, whereas other reported {Ni(NO)}¹⁰ complexes are neutral or cationic and are not bound by thiolates.

Of the structurally characterized, four-coordinate, monometallic {Ni(NO)}¹⁰ complexes, only two are supported by sulfur

- (31) Enemark, J. H.; Feltham, R. D. *J. Am. Chem. Soc.* **1974**, *96*, 5002–5004.
- (32) Schebler, P. J.; Riordan, C. G.; Guzei, I. A.; Rheingold, A. L. *Inorg. Chem.* **1998**, *37*, 4754–4755.
- (33) Fullmer, B. C.; Pink, M.; Fan, H.; Yang, X.; Baik, M.-H.; Caulton, K. G. *Inorg. Chem.* **2008**, *47*, 3888–3892.
- (34) Landry, V. K.; Pang, K.; Quan, S. M.; Parkin, G. *Dalton Trans.* **2007**, 820–824.
- (35) Landry, V. K.; Parkin, G. *Polyhedron* **2007**, *26*, 4751–4757.
- (36) Maffett, L. S.; Gunter, K. L.; Kreisel, K. A.; Yap, G. P. A.; Rabinovich, D. *Polyhedron* **2007**, *26*, 4758–4764.
- (37) MacBeth, C. E.; Thomas, J. C.; Betley, T. A.; Peters, J. C. *Inorg. Chem.* **2004**, *43*, 4645–4662.
- (38) Rahman, A. F. M. M.; Salem, G.; Stephens, F. S.; Wild, S. B. *Inorg. Chem.* **1990**, *29*, 5225–5230.
- (39) Krieger-Simonsen, J.; Elbaze, G.; Dartiguenave, M.; Feltham, R. D.; Dartiguenave, Y. *Inorg. Chem.* **1982**, *21*, 230–236.
- (40) Chong, K. S.; Rettig, S. J.; Storr, A.; Trotter, J. *Can. J. Chem.* **1979**, *57*, 3107–3112.
- (41) Di Vaira, M.; Ghilardi, C. A.; Sacconi, L. *Inorg. Chem.* **1976**, *15*, 1555–1561.
- (42) Meiners, J. H.; Rix, C. J.; Clardy, J. C.; Verkade, J. G. *Inorg. Chem.* **1975**, *14*, 705–710.
- (43) Enemark, J. H. *Inorg. Chem.* **1971**, *10*, 1952–1957.
- (44) Chen, Y.; Irie, Y.; Keung, W. M.; Maret, W. *Biochemistry* **2002**, *41*, 8360–8367.
- (45) Dicks, A. P.; Williams, D. L. H. *Chem. Biol.* **1996**, *3*, 655–659.
- (46) Kelm, M. *Biochim. Biophys. Acta* **1999**, *1411*, 273–289.
- (47) Singh, S. P.; Wishnok, J. S.; Keshive, M.; Deen, W. M.; Tannenbaum, S. R. *Proc. Natl. Acad. Sci. U.S.A.* **1996**, *93*, 14428–14433.
- (48) Tsikas, D.; Frölich, J. C. *Nitric Oxide* **2004**, *11*, 209–213.
- (49) Vanin, A. F.; Papina, A. A.; Serezhnikov, V. A.; Koppenol, W. H. *Nitric Oxide* **2004**, *10*, 60–73.
- (50) Bonner, L.; Stedman, G. In *Methods in Nitric Oxide Research*; Feelisch, M., Stamler, J. S., Eds.; Wiley: London, 1996; pp 4–18.

donor ligands (Chart 1).^{32,36} For comparison, the structural parameters for these complexes and their ν_{NO} values are reported in Table 2. Complexes **IIa,b** both contain $\{\text{Ni}(\text{NO})\}^{10}$ cores supported by monoanionic, $\kappa^3\text{-S}_3$ ligands and are arranged according to increasing ν_{NO} . Unfortunately, no clear trends are apparent in this comparison. Complex **2** most closely resembles **IIa** on the basis of the M–N bond length and the S–M–N and S–M–S angles. However, the N–O and M–S distances in **2** are most similar to those in **IIb**, whereas the Ni–N–O angle and solid-state NO stretching energy are substantially different from those of the other complexes with $\{\text{Ni}(\text{NO})\}^{10}$ cores bound to three sulfur atoms. A similar lack of any straightforward trend in structural parameters is also observed for manganese nitrosyls,⁵¹ for which the ν_{NO} is recommended as the most reliable measure of the $\{\text{M}(\text{NO})\}$ electron count. Complexes containing $\{\text{Cu}(\text{NO})\}^{11}$ cores are very rare, and the structurally characterized examples with C_{3v} geometries exhibit ν_{NO} values ranging from 1698 to 1742 cm^{-1} (avg = 1712 \pm 18 cm^{-1}).^{52,53} Because $\{\text{Cu}(\text{NO})\}^{11}$ formally contains one more electron in the metal nitrosyl unit than $\{\text{Ni}(\text{NO})\}^{10}$, complexes with this unit should display lower ν_{NO} values. This behavior is observed for the average NO stretching energies for $\{\text{Cu}(\text{NO})\}^{11}$ and $\{\text{Ni}(\text{NO})\}^{10}$ complexes with similar geometries (1712 vs 1742 cm^{-1}). However, complex **2** exhibits a ν_{NO} value in KBr nearly 50 cm^{-1} lower than the lowest measured value for a $\{\text{Cu}(\text{NO})\}^{11}$ complex, despite the latter having greater electron density within the metal nitrosyl unit. These results suggest that the electronic properties of a $\{\text{M}(\text{NO})\}$ core depend heavily on the electron-donating ability of the ligands and the overall charge of the molecule.

Interestingly, **2** has structural characteristics similar to those of the MNIC $(\text{Et}_4\text{N})[\text{Fe}(\text{NO})(\text{SPh})_3]$ (**IIc**, Table 2).⁹ The most notable differences between the two structures are a more acute M–N–O angle in **2**, a greater average M–S distance (2.301 vs 2.271 Å), and a more acute average S–M–S angle (102.7° vs 107.2°). These differences are consistent with the fact that **2** contains a $\{\text{Ni}(\text{NO})\}^{10}$ core and **IIc** a $\{\text{Fe}(\text{NO})\}^7$ core; greater electron density in the $\{\text{M}(\text{NO})\}$ unit will result in more π -backbonding. As the backbonding increases, the nitrosyl will become more reduced and adopt a more bent geometry. Furthermore, as the M–N bond develops multiple bonding character, its length will decrease, and the thiolates will be pulled closer together and lie farther away from the metal atom.

Synthesis and Properties of 3. Treatment of a solution of **1** in CH_3CN with 1 equiv of NOBF_4 produced an immediate color change from dark red to brown-green. Product and mass balance analysis revealed that 1 equiv of Ph_2S_2 , 1 equiv of Et_4NBF_4 , and 0.5 equiv of $(\text{Et}_4\text{N})_2[\text{Ni}_2(\text{NO})_2(\mu\text{-SPh})_2(\text{SPh})_2]$ (**3**) were produced per equiv of **1** consumed (Scheme 1). Complex **3** is also diamagnetic, and ^1H NMR spectroscopy revealed a 1:2 ratio of Et_4N^+ to PhS^- protons. Despite the presence of both terminal and bridging thiolate ligands in **3**, only one set of broadened aryl peaks was observed, presumably due to rapid exchange (Table 1). To test this hypothesis, the ^1H NMR spectrum of a 1:1 mixture of **2** and **3** was acquired, which revealed a single set of sharp aryl resonances at chemical shift values between

those of **2** and **3** (Figure S1), equal to the weighted average of their values in **2** and **3**, confirming that intermolecular thiolate exchange is occurring. The presence of only one set of broadened aryl peaks in the spectrum of **3** therefore results from a similar intermolecular exchange. Presumably, this process allows for isolation of crystalline **2** from a cooled THF solution of **3** and accounts for the interconversion of **2** and **3** by loss or gain of Et_4NSPh (vide infra).

In the solid state (KBr), only one NO stretch is observed for **3** at 1709 cm^{-1} , but in THF solution, **3** displays two NO stretching modes at 1751 and 1721 cm^{-1} . Like **2**, complex **3** contains a $\{\text{Ni}(\text{NO})\}^{10}$ core, and dimetallic complexes of this unit have been previously reported. There are examples of structurally characterized diamagnetic complexes comprising two $\{\text{Ni}(\text{NO})\}^{10}$ moieties bridged by anionic^{54–56} or neutral⁵⁷ ligands with NO stretching frequencies ranging from 1718 to 1817 cm^{-1} (avg = 1771 \pm 29 cm^{-1}). Furthermore, some of these complexes display one ν_{NO} value in the solid state and two in solution.⁵⁶ For example, the $[\text{Ni}_2(\text{NO})_2(\mu\text{-N}_2\text{C}_5\text{H}_7)_2\text{-}(\text{PPh}_3)_2]$ dimer, consisting of two $\{\text{Ni}(\text{NO})\}^{10}$ units bridged by 3,5-dimethylpyrazolates, exhibits one NO stretching mode at 1728 cm^{-1} in a Nujol mull and two at 1804 and 1758 cm^{-1} in cyclohexane solution. The solid-state IR spectrum of **3** suggests a C_i geometric configuration with *anti* nitrosyls and *trans* bridging thiolates. Only this arrangement of nitrosyl and thiolate ligands would afford an IR spectrum with one NO stretching band, of A_u symmetry. The other possible arrangements, *anti* nitrosyls and *cis* thiolates (C_s), *syn* nitrosyls and *cis* thiolates (C_{2v}), or *syn* nitrosyls and *trans* thiolates (C_s), are expected to display two IR-active NO stretching modes. Dipole–dipole interaction between solvent and **3** may allow the symmetric (A_g) stretching mode to become IR-active, or a different nitrosyl/thiolate geometric arrangement may be preferred in solution.

Reaction of **2** with 1 equiv of Me_3OBF_4 in CH_3CN yielded 0.5 equiv of **3** and 1 equiv of Et_4NBF_4 (Scheme 1). Because no Ph_2S_2 is formed, we presume that Me_3OBF_4 converts one PhS^- ligand to MeSPh , which cannot not be isolated or quantified due to its volatility. Additionally, cooling a saturated solution of **3** in THF to -30°C afforded **2**. This result is not surprising, given that **2** is THF-insoluble and could be formed by simple association of Et_4NSPh with **3**. Complex **2** could be formed in this manner by disproportionation of **3** into 1 equiv of **2** and 1 equiv of a molecule with the empirical formula $[\text{Ni}(\text{NO})(\text{SPh})]$. Even if the equilibrium favors **3**, **2** will selectively crystallize from THF solution, and its generation will be irreversible. Qualitative IR analysis of the reaction of **3** with Et_4NSPh similarly indicated formation of **2**.

Crystals suitable for X-ray diffraction were grown from vapor diffusion of Et_2O into a solution of **3** in CH_3CN at -30°C over 3 days. The structure confirms the assignment of **3** as containing a thiolate-bridged dimer of two $\{\text{Ni}(\text{NO})\}^{10}$ units (Figure 2). The nickel nitrosyl structural parameters for **3**, Ni–N–O = 161.5(2)°, N–O = 1.168(3) Å, Ni–N = 1.657(2) Å (Table 3), fall close to or within the range of values reported for analogous complexes containing two $\{\text{Ni}(\text{NO})\}^{10}$ cores bridged by anionic or neutral ligands (Ni–N–O = 166.4–178.9°,

(51) Ghosh, K.; Eroy-Reveles, A. A.; Avila, B.; Holman, T. R.; Olmstead, M. M.; Mascharak, P. K. *Inorg. Chem.* **2004**, *43*, 2988–2997.

(52) Fujisawa, K.; Tateda, A.; Miyashita, Y.; Okamoto, K.-i.; Paulat, F.; Praneeth, V. K. K.; Merkle, A.; Lehnert, N. *J. Am. Chem. Soc.* **2008**, *1205*–1213.

(53) Ruggiero, C. E.; Carrier, S. M.; Antholine, W. E.; Whittaker, J. W.; Cramer, C. J.; Tolman, W. B. *J. Am. Chem. Soc.* **1993**, *115*, 11285–11298.

(54) Heinemann, F. W.; Pritzkow, H.; Zeller, M.; Zenneck, U. *Organometallics* **2000**, *19*, 4283–4288.

(55) Chong, K. S.; Rettig, S. J.; Storr, A.; Trotter, J. *Can. J. Chem.* **1979**, *57*, 3099–3106.

(56) Chong, K. S.; Rettig, S. J.; Storr, A.; Trotter, J. *Can. J. Chem.* **1979**, *57*, 3090–3098.

(57) Del Zotto, A.; Mezzetti, A.; Novelli, V.; Rigo, P.; Lanfranchi, M.; Tiripicchio, A. *J. Chem. Soc., Dalton Trans.* **1990**, 1035–1042.

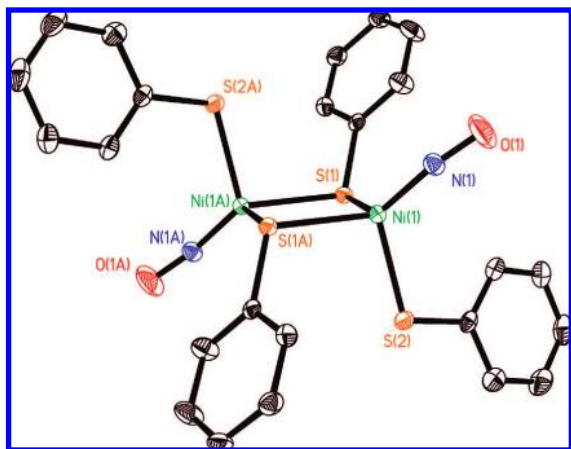


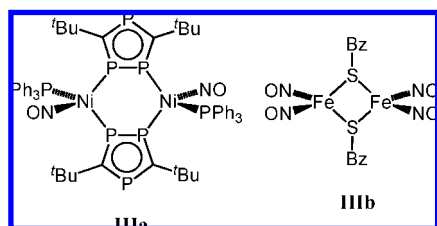
Figure 2. ORTEP diagram showing 50% probability thermal ellipsoids and selected atom labels for **3**. The Et₄N⁺ cations, H atoms, and disordered CH₃CN have been omitted for clarity. Selected bond distances (Å) and angles (deg): N1–O1, 1.168(3); Ni1–N1, 1.657(2); Ni1–S1, 2.2923(9); Ni1–S1A, 2.3320(10); Ni1–S2, 2.2733(11); Ni1–N1–O1, 161.5(2); S1–Ni1–N1, 118.56(8); S1A–Ni1–N1, 127.12(9); S2–Ni1–N1, 116.58(8); S1–Ni1–S1A, 89.24(4); S1–Ni1–S2, 100.80(3); S1A–Ni1–S2, 98.65(3).

Table 3. List of Bond Lengths (Å), Angles (deg), and ν_{NO} (cm⁻¹) Values for **3** and **IIIa,b**^a

	3	IIIa	IIIb
N–O	1.168(3)	1.169(5)	1.161(2)
M–N	1.657(2)	1.662(3)	1.6725(16)
M–A _t	2.2733(11)	2.3304(11)	–
M–A _b	2.3320(10)	2.2874(11)	2.2569(5)
	2.2923(9)	2.2626(11)	2.2527(5)
M–N–O	161.5(2)	166.4(3)	167.0(2)
A _t –M–N	116.58(8)	124.56(12)	–
A _b –M–N	127.12(9)	111.67(12)	108.91(6)
	118.56(8)	107.44(12)	107.73(8)
A _b –M–A _t	100.80(3)	105.50(4)	–
	98.65(3)	103.54(4)	–
A _b –M–A _b	89.24(4)	101.74(4)	106.060(17)
ν _{NO} (solid)	1709	1751	1775, 1749
ν _{NO} (soln)	1751, 1721	–	1783, 1765, 1722

^a A_t = atom coordinated to metal from terminal, non-nitrosyl ligand. A_b = atom coordinated to metal from bridging, non-nitrosyl ligand.

Chart 2



avg = 172.6 ± 5.4°; N–O = 1.13–1.183 Å, avg = 1.154 ± 0.024 Å; Ni–N = 1.591–1.670 Å, avg = 1.638 ± 0.033 Å).^{54–57} There are no examples of dimers of {Ni(NO)}¹⁰ units supported by terminal or bridging thiolates. The closest analogue of **3** that has been structurally characterized (**IIIa**, Chart 2) contains two {Ni(NO)}¹⁰ cores bridged by two triphospholyl ligands (Table 3).⁵⁴ Although the bridging and terminal ligands are different and **3** is dianionic whereas **IIIa** is neutral, the average bond lengths are nearly identical. However, the average S–Ni–N angle in **3** (120.8°) is more obtuse than the average P–Ni–N angle in **IIIa** (114.6°), and the average S–Ni–S angle in **3** is more acute than the average P–Ni–P angle in **IIIa**

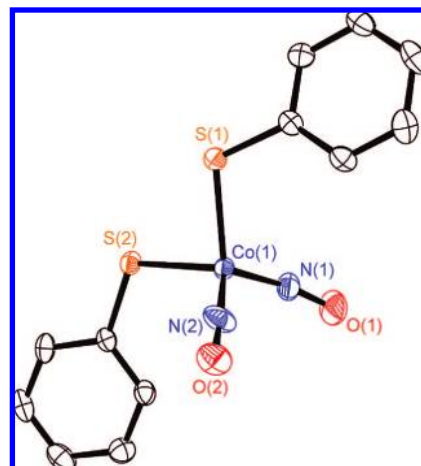
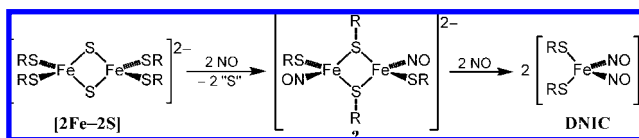


Figure 3. ORTEP diagram showing 50% probability thermal ellipsoids and selected atom labels for **5**. The Et₄N⁺ cation and H atoms have been omitted for clarity. Selected bond distances (Å) and angles (deg): N1–O1, 1.106(3); N2–O2, 1.126(3); Co1–N1, 1.684(3); Co1–N2, 1.651(3); Co1–S1, 2.2478(8); Co1–S2, 2.2565(8); Co1–N1–O1, 161.4(3); Co1–N2–O2, 174.9(2); N1–Co–N2, 110.35(14); S1–Co1–N1, 111.56(9); S1–Co1–N2, 118.38(9); S2–Co1–N1, 116.26(9); S2–Co1–N2, 111.67(10); S1–Co1–S2, 87.14(3).

Scheme 2. Proposed Conversion of a [2Fe–2S] Cluster into DNICs



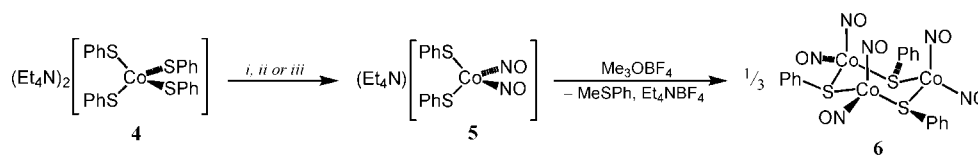
(96.23° vs 103.6°). Although both **3** and **IIIa** contain dimers of {Ni(NO)}¹⁰ cores, complex **3** has an overall 2– charge and is supported by thiolate ligands. As a result, the nickel atom in **3** will be more electron-rich than in **IIIa**, resulting in greater π-backbonding.

Although no iron analogue of **3** is known, the structure of **3** suggests a possible intermediate in the conversion of 1 equiv of [Fe₂S₂(SR)₂]^{2–} to 2 equiv of the DNIC [Fe(NO)₂(SR)₂][–]. This process requires a net gain of 4 equiv of NO and a net loss of 2 equiv of sulfur, of unknown allotropic form. Coordination of 2 equiv of NO followed by extrusion of sulfur might afford [Fe₂(NO)₂(μ-SR)₂(SR)₂]^{2–}, the iron analogue of **3**, composed of two {Fe(NO)}⁸ units stabilized by π-donating thiolate ligands (Scheme 2). Subsequent binding of 1 equiv of NO to each metal could break apart the dimer to yield 2 equiv of DNIC. Preliminary experiments performed in our laboratory have suggested that such an intermediate exists.⁵⁸ This observation suggests a possible intermediate in the breakdown of [2Fe–2S] clusters into DNICs in vivo.

Crystal structures of Roussin red ester (RRE) complexes of the general formula [Fe₂(NO)₄(μ-SR)₂] have been known for decades.⁵⁹ For comparison, we have juxtaposed the structural parameters of **3** with those previously obtained for the RRE [Fe₂(NO)₄(μ-SBz)₂] (**IIIb**) in Table 3.⁸ The M–N and N–O bond lengths are nearly identical, whereas the bridging thiolate–metal bonds are slightly longer in **3** than in **IIIb** (2.3122 vs 2.2548 Å). Unsurprisingly, the M–N–O angle is more acute in **3** than in **IIIb**. Because **3** contains a {Ni(NO)}¹⁰

(58) Harrop, T. C.; Lippard, S. J., unpublished results.

(59) Thomas, J. T.; Robertson, J. H.; Cox, E. G. *Acta Crystallogr.* **1958**, *11*, 599–604.

Scheme 3. Syntheses of **5** and **6**^a

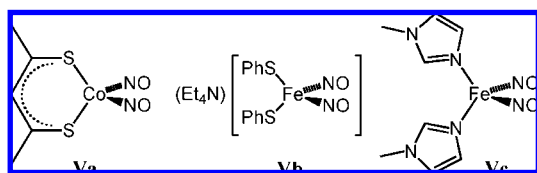
^a (i) +2 equiv of Ph₃CSNO, -1.5 equiv of R₂S₂ and 1 equiv of Et₄N⁺SPH⁻; (ii) +excess NO(g), -0.5 equiv of Ph₂S₂ and 1 equiv of Et₄N⁺SPH⁻; (iii) +1 equiv of NOBF₄, -0.5 equiv of Ph₂S₂ and 1 equiv of Et₄NBF₄ (to afford 0.5 equiv of **5**).

Table 4. List of Bond Lengths (Å), Angles (deg), and ν_{NO} (cm⁻¹) Values for **5** and Va–c

	5	Va ^a	Vb	Vc
N–O	1.126(3) 1.106(3)	1.120(5)	1.181(2) 1.179(2)	1.189(3) 1.188(4)
M–N	1.684(3) 1.651(3)	1.650(6)	1.680(2) 1.678(2)	1.650(3) 1.648(3)
M–S	2.2565(8) 2.2478(8)	2.224(2) 2.217(2)	2.288(1) 2.272(1)	—
M–N–O	174.9(2) 161.4(3)	168.9(5)	169.4(2) 168.5(2)	170.1(3) 167.5(3)
N–M–N	110.35(14)	115.5(3)	117.36(9)	117.33 ^b
S–M–N	118.38(9) 116.26(9) 111.67(10) 111.56(9)	111.1(2) 109.1(2)	111.47(6) 110.81(6) 103.88(6) 103.61(6)	—
S–M–S	87.14(3)	100.0(1)	109.73(2)	—
ν_{NO} (solid)	1756, 1678	—	1743, 1683	—
ν_{NO} (soln)	1769, 1699	1820, 1750	1737, 1693	1673, 1617

^a Structural parameters averaged for metal nitrosyl moieties in original report with errors propagated. ^b For the nitrosyl nitrogens.

Chart 3



core, there are more electrons spread over fewer NO moieties than in the {Fe(NO)₂}⁹ complex, and therefore π -backbonding is better. The greater multiple-bond character between the metal and nitrosyl in **3** shortens the M–N bond with concomitant lengthening of the M–S bonds. One nitrosyl will cause the three other ligands in a pseudotetrahedral configuration to draw closer together; two nitrosyls will prefer a wider separating angle and cause the bridging thiolates to spread farther apart. An additional difference between **3** and **IIIb** is the ability of the two {Fe(NO)₂}⁹ units in the latter to interact via an Fe–Fe bond, which is not possible for two {Ni(NO)}¹⁰ units.

Attempts to prepare a nickel dinitrosyl complex by reacting **2** with NO(g) or Ph₃CSNO failed, yielding only slow conversion to **3**. This result is consistent with the fact that there are no structurally characterized complexes containing a {Ni(NO)₂}ⁿ fragment of any electron count. As *n* increases above 10 electrons, M–NO antibonding orbitals would become filled and cause dissociation of one of the nitrosyl ligands. For *n* to be less than or equal to 10 electrons with nickel, the metal would need to be in a 2+ oxidation state, an electronic configuration not conducive to supporting two nitrosyl ligands. Other metals, such as iron and cobalt, can support two nitrosyl ligands in a 1+ oxidation state without exceeding *n* = 10.

Synthesis and Properties of the First Mononuclear {Co(NO)₂}¹⁰ Anion (5**).** Upon addition of 2 equiv of Ph₃CSNO to a solution of **4** in CH₃CN, the solution color immediately changed from

dark green to dark brown. Mass balance analysis revealed that 1.5 equiv of disulfide, 1 equiv of Et₄N⁺SPH⁻, and 1 equiv of (Et₄N)[Co(NO)₂(SPh)₂] (**5**) were produced per equiv of **4** consumed (Scheme 3, route *i*). Complex **5** is diamagnetic, and its ¹H NMR spectrum displays a 1:2 ratio of Et₄N⁺ to PhS⁻ protons (Table 1). The asymmetric and symmetric NO stretching modes for **5** occur at 1678 and 1756 cm⁻¹ in the solid state (KBr) and shift to 1699 and 1769 cm⁻¹ in solution (THF), respectively.

Complex **5** contains a {Co(NO)₂}¹⁰ core, and other four-coordinate, monometallic complexes with this configuration have asymmetric ν_{NO} values ranging from 1730 to 1798 cm⁻¹ (avg = 1766 ± 20 cm⁻¹) and symmetric ν_{NO} values ranging from 1809 to 1870 (avg = 1837 ± 18 cm⁻¹).^{60–66} Presumably, the asymmetric and symmetric ν_{NO} modes for **5** are nearly 100 cm⁻¹ lower than the average values observed with other {Co(NO)₂}¹⁰ complexes because the previously reported complexes of this configuration have been overall charge neutral or cationic. Complex **5** represents the first example of a {Co(NO)₂}¹⁰ species contained within an anion. The formation of **5** from **4** may proceed through a cobalt mononitrosyl intermediate, but attempts to observe such a species by IR or UV–vis spectroscopy were unsuccessful. Addition of fewer than 2 equiv of NO(g) or Ph₃CSNO yields incomplete conversion to **5**.

As with the Ph₃CSNO reactivity, addition of excess NO(g) to **4** yielded 0.5 equiv of Ph₂S₂, 1 equiv of Et₄N⁺SPH⁻, and 1 equiv of **5** (Scheme 3, route *ii*). Surprisingly, addition of 1 equiv of NOBF₄ to a solution of **4** in CH₃CN yielded 0.5 equiv of Ph₂S₂, 1 equiv of Et₄NBF₄, and 0.5 equiv of **5**, as well as an intractable plum-colored solid, the IR spectrum of which showed bands only for the Et₄N⁺ and PhS⁻ moieties (Scheme 3, route *iii*). The combination of mass balance analysis and the IR spectrum of this material suggests it could have the formula (Et₄N)[Co(SPh)₄]. Such a product would be consistent with a possible mechanism by which **5** might form. Oxidation of **4** by NOBF₄ would yield 0.5 equiv of Ph₂S₂, 1 equiv of Et₄NBF₄, 1 equiv of NO, and 1 equiv of “(Et₄N)[Co(SPh)₃]”. Presumably, this cobalt(II) thiolate complex would rapidly bind NO to produce a cobalt(II) nitrosyl. Previous studies have demonstrated

(60) Lim, M. H.; Kuang, C.; Lippard, S. J. *ChemBioChem* **2006**, *7*, 1571–1576.

(61) Franz, K. J.; Singh, N.; Spingler, B.; Lippard, S. J. *Inorg. Chem.* **2000**, *39*, 4081–4092.

(62) Gerbase, A. E.; Vichi, E. J. S.; Stein, E.; Amaral, L.; Vasquez, A.; Hörner, M.; Maichle-Mössner, C. *Inorg. Chim. Acta* **1997**, *266*, 19–27.

(63) Roustan, J.-L.; Ansari, N.; Le Page, Y.; Charland, J.-P. *Can. J. Chem.* **1992**, *70*, 1650–1657.

(64) Aresta, M.; Ballivet-Tkatchenko, D.; Bonnet, M. C.; Faure, R.; Loiseleur, H. *J. Am. Chem. Soc.* **1985**, *107*, 2994–2995.

(65) Haymore, B. L.; Huffman, J. C.; Butler, N. E. *Inorg. Chem.* **1983**, *22*, 168–170.

(66) Kaduk, J. A.; Ibers, J. A. *Inorg. Chem.* **1977**, *16*, 3283–3287.

that [Co^{II}(NO)(L)] complexes disproportionate to form 0.5 equiv of [Co^I(NO)₂] and 0.5 equiv of [Co^{III}(L)₂].^{67,68}

Crystals suitable for X-ray diffraction were grown by cooling a saturated solution of **5** in THF to -30 °C overnight. The structure confirms the assignment of **5** as containing a {Co(NO)₂}¹⁰ fragment supported by two thiolates (Figure 3). The cobalt nitrosyl structural parameters for **5** (Co–N–O = 161.4(3)° and 174.9(2)°, N–Co–N = 110.35(14)°, N–O = 1.106(3) and 1.126(3) Å, Co–N = 1.651(3) and 1.684(3) Å, Table 4) fall close to or within the range of reported values for four-coordinate, monometallic {Co(NO)₂}¹⁰ complexes (Co–N–O = 162.2–176.6°, avg = 169.2 ± 4.9°; N–Co–N = 115.6–131.7°, avg = 121.7 ± 6.6°; N–O = 1.12–1.156 Å, avg = 1.142 ± 0.011 Å; Co–N = 1.641–1.671 Å, avg = 1.654 ± 0.010 Å). The cobalt dinitrosyl complex (**Va**) is the only structurally characterized, monometallic {Co(NO)₂}¹⁰ unit coordinated by sulfur atoms (Chart 3).⁶⁹ A summary of its bond lengths and angles is presented in Table 4. The average cobalt nitrosyl structural parameters for **5** are similar to those for **Va**, but the Co–S bonds are longer and the S–M–S angle is more acute. Presumably, the greater Co–S distances in **5** are due to increased electron density at the metal compared to **Va**. Although the smaller S–M–S angle in **5** may reflect greater π-backbonding from the metal to the nitrosyls compared to **Va**, the ligand supporting the latter complex is bidentate, and its geometry is dictated by the delocalized π-system. An idealized five-membered chelate ring would exhibit an S–M–S angle of 108°, and an idealized six-membered chelate ring would display an angle of 120°. Because five of the six atoms in the chelate ring for **Va** are sp²-hybridized, whereas the cobalt atom in **5** contains only monodentate ligands, the S–M–S angle in **Va** will be necessarily greater, independent of any electronic effects.

Although the NO stretching bands in **5** are well below the range of those reported for other complexes, the IR spectrum for the DNIC (Et₄N)[Fe(NO)₂(SPh)₂] (**Vb**) strongly resembles that of **5**. The average M–N distance in **5** is shorter than that in **Vb**, consistent with greater π-backbonding, but the N–O lengths are significantly shorter. A DNIC containing a {Fe(NO)₂}¹⁰ core supported by 1-methylimidazole ligands (**Vc**)⁷⁰ should be a better molecule for comparison to **5** because it has the same number of electrons in its {M(NO)₂} framework. However, the M–N bonds in **Vc** are shorter and the N–O distances are greater, suggesting more π-backbonding in **Vc** than **5**. Consistent with this speculation, the symmetric and asymmetric ν_{NO} values in **Vc** are nearly 100 cm⁻¹ lower in energy than those observed in **5**. Discussion of the electronic configuration of metal nitrosyl complexes based solely on structural parameters can be counterproductive, but the ν_{NO} values should be consistent with the Enemark–Feltham configuration of the complex. Perhaps the use of σ,π-donor thiolates negates the validity of considering the metal nitrosyl core as an independent moiety.

Synthesis and Properties of 6. Addition of stoichiometric Me₃OBf₄ to a solution of **5** in CH₃CN caused an immediate color change from dark brown to dark red-orange. Product and

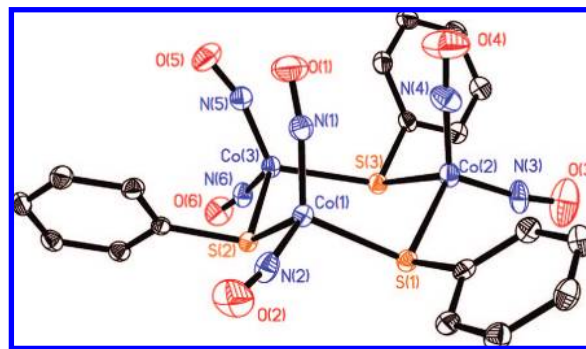


Figure 4. ORTEP diagram showing 50% probability thermal ellipsoids and selected atom labels for **6**. The H atoms have been omitted for clarity. Selected bond distances (Å) and angles (deg): N1–O1, 1.139(4); N2–O2, 1.131(4); N3–O3, 1.135(4); N4–O4, 1.127(4); N5–O5, 1.154(4); N6–O6, 1.147(4); Co1–N1, 1.663(3); Co1–N2, 1.675(3); Co2–N4, 1.668(3); Co3–N5, 1.674(3); Co3–N6, 1.669(3); Co1–S1, 2.3093(9); Co1–S2, 2.2814(9); Co2–S1, 2.2832(9); Co2–S3, 2.2811(10); Co3–S2, 2.2984(9); Co3–S3, 2.3027(9); Co1–N1–O1, 170.2(3); Co1–N2–O2, 171.1(3); Co2–N3–O3, 170.1(3); Co2–N4–O4, 175.8(3); Co3–N5–O5, 164.3(3); Co3–N6–O6, 173.0(3); N1–Co1–N2, 119.30(5); N3–Co2–N4, 118.05(16); N5–Co3–N6, 119.60(14); S1–Co1–N1, 114.97(10); S1–Co1–N2, 110.72(10); S1–Co2–N3, 111.86(11); S1–Co2–N4, 112.51(11); S2–Co1–N1, 106.97(10); S2–Co1–N2, 106.88(10); S2–Co3–N5, 102.13(10); S2–Co3–N6, 107.40(10); S3–Co2–N3, 102.36(11); S3–Co2–N4, 111.66(11); S3–Co3–N5, 121.29(10); S3–Co3–N6, 105.12(10); S1–Co1–S2, 94.59(3); S1–Co2–S3, 98.07(4); S2–Co3–S3, 98.22(3).

mass balance analyses indicated that 1 equiv of Et₄NBF₄ and 1/3 equiv of [Co₃(NO)₆(μ-SPh)₃] (**6**) were formed per equiv of **5** consumed (Scheme 3). Compound **6** is diamagnetic, and ¹H NMR spectroscopy reveals only PhS⁻ protons (Table 1). The NO stretches of **6** occur at 1840, 1817, 1779, and 1744 cm⁻¹ in the solid state (KBr). The ν_{NO} values in THF solution do not shift significantly and appear at 1844, 1819, 1780, and 1764 cm⁻¹. Both solid-state and solution ν_{NO} values for **6** lie within the range of values previously observed for complexes comprising one {Co(NO)₂}¹⁰ unit (vide supra) or multiple ligand-bridged {Co(NO)₂}¹⁰ units (1750–1878 cm⁻¹, avg = 1815 ± 41 cm⁻¹).^{71–74} Synthesis of a *dimetallic* [Co₂(NO)₄(μ-SPh)₂] compound from [Co₂(NO)₄(μ-Cl)₂] and LiSPh has been reported.⁷⁵ Although the NO stretches at 1842, 1820, 1783, and 1767 cm⁻¹ in this complex are nearly identical to those observed for **6**, the only other characterization provided was its mass spectrum. In the solid state, **6** displays C_{3v} symmetry (Figure 4, see below), and its six nitrosyls should give rise to four IR-active modes (2A₁ + 2E), as we observe. If **6** were a dimetallic species with the same solid-state structure as RRE (C_{2h}), only two NO stretching modes would be IR-active (A_g + B_u). Because four overlapping NO stretching bands are observed in the solid-state and solution IR, we conclude that the trimetallic formulation is retained in solution. The ν_{NO} values for **6** are in excellent agreement with those reported for the purported [Co(NO)₂(μ-SR)]_n complexes.⁷⁵

Crystals suitable for X-ray diffraction were grown by cooling a saturated solution of **6** in Et₂O to -30 °C overnight. The

(67) Del Zotto, A.; Mezzetti, A.; Rigo, P. *Inorg. Chim. Acta* **1990**, *171*, 61–69.
 (68) Hendrickson, A. R.; Ho, R. K. Y.; Martin, R. L. *Inorg. Chem.* **1974**, *13*, 1279–1281.
 (69) Martin, R. L.; Taylor, D. *Inorg. Chem.* **1976**, *15*, 2970–2976.
 (70) Reginato, N.; McCrory, C. T. C.; Pervitsky, D.; Li, L. *J. Am. Chem. Soc.* **1999**, *121*, 10217–10218.

(71) Hilderbrand, S. A.; Lippard, S. J. *Inorg. Chem.* **2004**, *43*, 5294–5301.
 (72) Chong, K. S.; Rettig, S. J.; Storr, A.; Trotter, J. *Can. J. Chem.* **1979**, *57*, 3119–3125.
 (73) Strouse, C. E.; Swanson, B. I. *J. Chem. Soc., Chem. Commun.* **1971**, 55–56.
 (74) Dahl, L. F.; de Gil, E. R.; Feltham, R. D. *J. Am. Chem. Soc.* **1969**, *91*, 1653–1664.
 (75) Bitterwolf, T. E.; Pal, P. *Inorg. Chim. Acta* **2006**, *359*, 1501–1503.

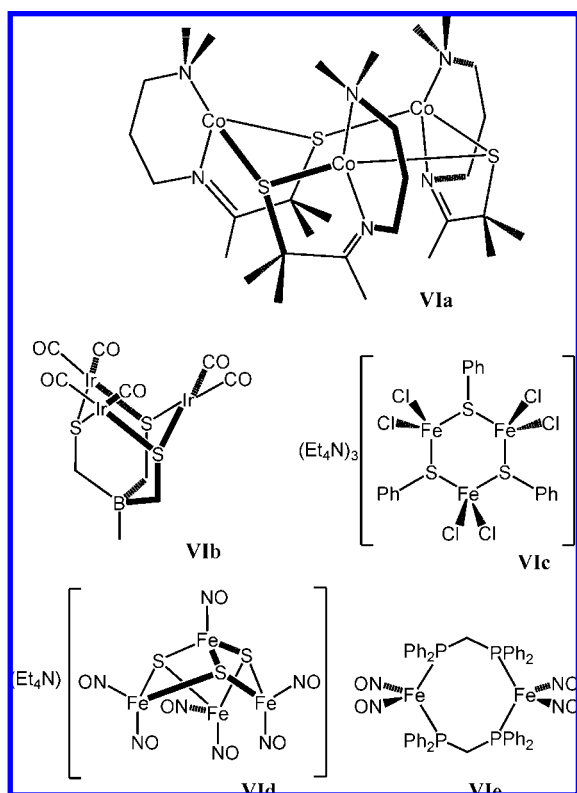
Table 5. List of Bond Lengths (Å), Angles (deg), and ν_{NO} (cm^{-1}) Values for **6** and **Vla–e**

	6 ^a	Vla ^a	Vlb ^a	Vlc ^a	Vld ^{a,b}	Vle ^a
N–O	1.139	—	—	—	1.162	1.19
M–N	1.670	—	—	—	1.669	1.650
M–S	2.293	2.292	2.369	2.356	2.256	—
M–N–O	170.8	—	—	—	166.4	171.7
N–M–N	119.0	—	—	—	115.3	116.9
S–M–N	109.49	—	—	—	110.4	—
S–M–S	96.96	132.61	94.8	100.5	104.07	—
ν_{NO} (solid)	1840, 1817, 1779, 1744	—	—	—	—	—
ν_{NO} (soln)	1844, 1819, 1780, 1764	—	—	—	1795, 1743 1708	1733, 1721 1687, 1668

^a Bond lengths and angles are averaged for all similar occurrences.

^b Excluding apical $\{\text{Fe}(\text{NO})\}_7$ unit.

Chart 4



structure reveals that **6** contains a trimer of thiolate-bridged $\{\text{Co}(\text{NO})_2\}^{10}$ fragments (Figure 4). The average bond lengths and angles for the $\{\text{Co}(\text{NO})_2\}^{10}$ units in **6** ($\text{N–Co–N} = 119.0^\circ$, $\text{Co–N–O} = 170.8^\circ$, $\text{N–O} = 1.139 \text{ \AA}$, $\text{Co–N} = 1.670 \text{ \AA}$, Table 5) fall within the range of reported values for four-coordinate, monometallic (vide supra) or multimetallic $\{\text{Co}(\text{NO})_2\}^{10}$ complexes ($\text{Co–N–O} = 161.6\text{--}173.5^\circ$, $\text{avg} = 168.2 \pm 5.1^\circ$; $\text{N–Co–N} = 109.8\text{--}118.3^\circ$, $\text{avg} = 112.5 \pm 3.2^\circ$; $\text{N–O} = 1.11\text{--}1.19 \text{ \AA}$, $\text{avg} = 1.146 \pm 0.022 \text{ \AA}$; $\text{Co–N} = 1.60\text{--}1.68 \text{ \AA}$, $\text{avg} = 1.648 \pm 0.030 \text{ \AA}$).^{71–74}

Although there are no structurally characterized complexes with three ligand-bridged $\{\text{Co}(\text{NO})_2\}^{10}$ units, dimers^{71,72} and infinite chains^{73,74} are known. Only one thiolate-bridged trimetallic complex containing four-coordinate cobalt centers (**VIa**) has been structurally characterized (Chart 4). Although the average Co–S lengths are similar, the average S–Co–S angle is wider in **VIa**, most likely due to the geometric constraints imposed by the ligand (Table 5).⁷⁶ A trimer of $\{\text{Ir}(\text{CO})_2\}$ units bridged by alkyl thiolates (**VIb**)⁷⁷ is a better structural analogue of the metal thiolate core in **6** and displays a comparable average

S–M–S angle; the greater average M–S length in **VIb** is most likely a consequence of the greater ionic radius of iridium (0.69 vs 0.82 Å for $\text{Co}(\text{III})$ vs $\text{Ir}(\text{III})$ in octahedral, high-spin configurations).⁷⁸ The M_3S_3 core of **VIb** also more closely resembles the cyclohexane-like configuration of **6** than does **VIa**.

Although no iron analogue of **6** has been reported, $(\text{Et}_4\text{N})_3\text{[Fe}_3\text{Cl}_6(\mu\text{-SPh})_3]$ (**VIc**) shares its M_3S_3 core configuration.⁷⁹ Despite having an average S–M–S angle similar to that in **6**, **VIc** exhibits a much longer M–S distance and a planar M_3S_3 core. An iron nitrosyl complex with structural parameters and ν_{NO} values similar to those in **6** is the Roussin black salt (RBS), $(\text{Et}_4\text{N})[\text{Fe}_4\text{S}_3(\text{NO})_7]$ (**VId**).⁸⁰ The greater average N–O distance in **VId** compared to **6**, the more acute average M–N–O angle and more obtuse S–M–S angle in **VId**, and the lower ν_{NO} values suggest that there is greater M–NO π -backbonding in **VId** than in **6**. Although **6** contains three $\{\text{Co}(\text{NO})_2\}^{10}$ units and **VId** three equatorial $\{\text{Fe}(\text{NO})_2\}^{10}$ units, the latter are bridged by sulfides and the complex is overall anionic, thus providing a more electron-rich environment for the metal centers in **VId**. An analogue of RRE containing $\{\text{Fe}(\text{NO})_2\}^{10}$ units bridged by two bis(diphenylphosphino)methane ligands (**VIe**)⁸¹ displays nearly identical metal nitrosyl angles, but the average M–N distance is shorter and the average N–O length is greater than in **6**, indicating better π -backbonding in **VIe**.

In support of this observation, the NO stretching energies in **VIe** are nearly 100 cm^{-1} lower in energy than those in **6**. Although **6** and **VIe** both contain $\{\text{M}(\text{NO})_2\}^{10}$ cores and the cobalt complex is supported by σ,π -donor ligands, the iron complex exhibits structural and spectroscopic parameters consistent with greater electron density residing within the M–NO units. Because **6** and **VIe** have the same Enemark–Feltham configuration, the iron must be in a more reduced state and will thus be more electron-releasing than the cobalt.

The results for the nickel and cobalt nitrosyls supported by thiolates, especially in comparison with similar metal nitrosyl thiolate complexes, suggest that the nature of the metal and supporting ligands can have a nontrivial influence on the structural and vibrational properties of the “independent” $\{\text{M}(\text{NO})_x\}^n$ core. Comparison to other complexes containing similar metal nitrosyl units has revealed the importance of the electron-donating ability of the ligand and the overall charge of the molecule in influencing the electronic properties of the metal nitrosyl core. These relationships are currently being explored via computational methods and will be reported at a later date.

NO Transfer to [Fe(TPP)Cl]. The metalloporphyrin $[\text{Fe}(\text{TPP})\text{Cl}]$ can be used to measure the ability of a metal nitrosyl complex to donate or transfer NO by monitoring the response of the Soret band at 417 nm.^{8,82} The reaction between $[\text{Fe}$

(76) Shearer, J.; Kaminsky, W.; Kovacs, J. A. *Acta Crystallogr. C* **2003**, *59*, m379–m380.

(77) Maisonnat, A.; Devillers, J.; Poilblanc, R. *Inorg. Chem.* **1987**, *26*, 1502–1507.

(78) Cotton, F. A.; Wilkinson, G.; Murillo, C. A.; Bochmann, M. *Advanced Inorganic Chemistry*, 6th ed.; John Wiley & Sons, Inc.: New York, 1999.

(79) Whitener, M. A.; Bashkin, J. K.; Hagen, K. S.; Girerd, J.-J.; Gamp, E.; Edelstein, N.; Holm, R. H. *J. Am. Chem. Soc.* **1986**, *108*, 5607–5620.

(80) D’Addario, S.; Demartin, F.; Grossi, L.; Iapalucci, M. C.; Laschi, F.; Longoni, G.; Zanello, P. *Inorg. Chem.* **1993**, *32*, 1153–1160.

(81) Li, L.; Reginato, N.; Urschey, M.; Stradiotto, M.; Liarakos, J. D. *Can. J. Chem.* **2003**, *81*, 468–475.

(82) Chiang, C.-Y.; Darensbourg, M. Y. *J. Biol. Inorg. Chem.* **2006**, *11*, 359–370.

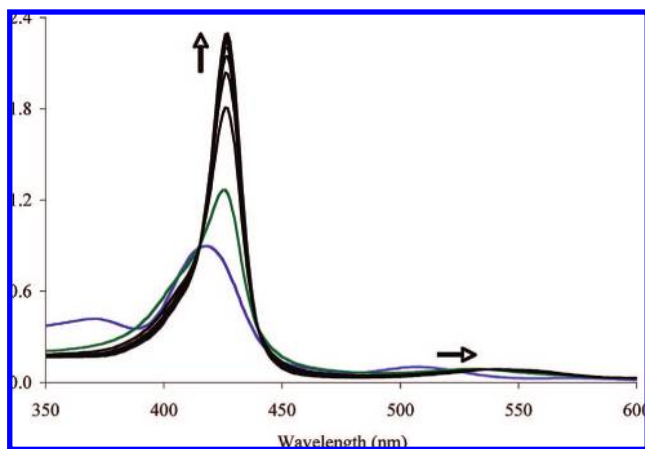


Figure 5. Reaction of $[\text{Fe}(\text{TPP})\text{Cl}]$ with **2** in THF without illumination. The Soret band for $[\text{Fe}(\text{TPP})\text{Cl}]$ (purple trace) shifts hypsochromically and increases in intensity upon addition of **2** (green trace). Scans every 60 s thereafter (black traces) show increasing absorptivity that is complete within 10 min.

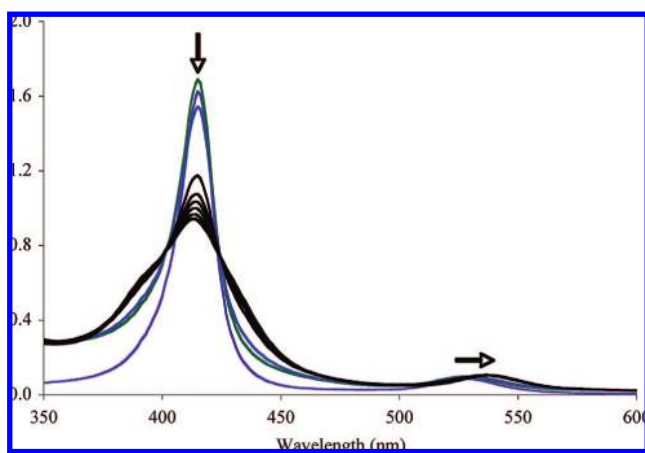


Figure 6. Reaction of $[\text{Co}(\text{TPP})]$ with **2** in THF with illumination. The Soret band for $[\text{Co}(\text{TPP})]$ (purple trace) is unaffected by the addition of **2** (green trace). After 60 s of exposure to ambient lighting, the intensity had decreased (blue trace). Scans every 5 min thereafter (black traces) show decreasing absorptivity that is complete within 30 min.

(TPP)Cl] and the MNIC $(\text{Et}_4\text{N})[\text{Fe}(\text{NO})(\text{S}'\text{Bu})_3]$ under ambient fluorescent lighting afforded $[\text{Fe}(\text{TPP})(\text{NO})]$ with the expected hypsochromic shift to 405 nm and small decrease in absorptivity. However, $[\text{Fe}(\text{TPP})(\text{NO})]$ is only obtained by reductive nitrosylation of $[\text{Fe}(\text{TPP})\text{Cl}]$ — an exogenous electron must be supplied, with the displaced chloride being trapped by the NO donor.²⁴ In the absence of a reducing agent, reaction of a stoichiometric amount of NO(g) with $[\text{Fe}(\text{TPP})\text{Cl}]$ in aprotic solvent affords $[\text{Fe}(\text{TPP})(\text{NO})\text{Cl}]$, a complex that is optically indistinguishable from $[\text{Fe}(\text{TPP})\text{Cl}]$.²⁴ When solutions of this six-coordinate nitrosyl are allowed to stand, they gradually lose NO and the spectrum of the original $[\text{Fe}(\text{TPP})\text{Cl}]$ is restored, and this process is greatly accelerated upon exposure to a vacuum.

Contrary to our expectations, addition of 1 equiv of **2**, 0.5 equiv of **3**, or 1 equiv of **5** to $[\text{Fe}(\text{TPP})\text{Cl}]$ in THF produced a *bathochromic* shift in the Soret band from 417 to 426 nm with dramatic increases in absorption *in the dark* (Figure 5). Because the Soret band moves to lower energy and the absorptivity increases, we can exclude the formation of either $[\text{Fe}(\text{TPP})(\text{NO})\text{Cl}]$ or $[\text{Fe}(\text{TPP})(\text{NO})]$. Iron porphyrin nitrosyl complexes

have been extensively studied, and coordination of a sixth ligand to $[\text{Fe}(\text{TPP})(\text{NO})]$ can cause a significant change in the optical spectrum.

The six-coordinate $[\text{Fe}(\text{TPP})(\text{NO})(\text{MeIm})]$ complex, where MeIm is 1-methylimidazole, has a Soret band at 425 nm with $\epsilon = 1.54 \times 10^6 \text{ M}^{-1} \text{ cm}^{-1}$.⁸³ However, product analysis from a preparative-scale reaction of **2** with $[\text{Fe}(\text{TPP})\text{Cl}]$ revealed an IR spectrum identical to that of **3** and no evidence for formation of Ph_2S_2 . We therefore conclude that **2** transfers PhS^- to $[\text{Fe}(\text{TPP})\text{Cl}]$ with concomitant formation of **3** and Et_4NCl . Because **3** and **5** have the same optical response, we propose that these complexes also undergo thiolate–chloride ligand exchange.

NO Transfer to $[\text{Co}(\text{TPP})]$. To avoid the mechanistic complications of $[\text{Fe}(\text{TPP})\text{Cl}]$, we studied the ability of one of our nitrosyl complexes to transfer NO to $[\text{Co}(\text{TPP})]$. Addition of **2** to $[\text{Co}(\text{TPP})]$ in THF did not significantly alter the optical spectrum when shielded from light. A small increase in intensity of the Soret band was noted due to the absorption of **2** at this wavelength. Exposure of the $[\text{Co}(\text{TPP})] + \text{2}$ solution to ambient fluorescent lighting after 60 s and at 5 min intervals thereafter produced a rapid decrease in absorption along with a slight hypsochromic shift (Figure 6). The final spectrum obtained from this reaction matched that for $[\text{Co}(\text{TPP})] + \text{NO}(\text{g})$ or Ph_3CSNO but not the previously reported values for the Soret band wavelength and absorptivity of $[\text{Co}(\text{TPP})(\text{NO})]$.²⁷ As a control, the reaction of $[\text{Co}(\text{TPP})]$ with Ph_3CSNO was performed on a preparative scale, and the ν_{NO} value observed was 1697 cm^{-1} . This value is in good agreement with that previously observed for $[\text{Co}(\text{TPP})(\text{NO})]$. The cause of the disparity between the results from IR and UV–vis spectroscopy is unclear, but the optical spectrum of $[\text{Co}(\text{TPP})(\text{NO})]$ may depend on solvent, since our measurements were performed in THF and the literature values²⁷ were acquired in CH_2Cl_2 . By comparison, cobalt(II)-reconstituted soluble guanylyl cyclase displays a slight hypsochromic shift in the Soret band upon coordination of NO with a decrease in absorptivity to $1.07 \times 10^5 \text{ M}^{-1} \text{ cm}^{-1}$.²⁸

Conclusions and Speculations

Reaction of **1** with Ph_3CSNO or NO(g) yielded the monometallic $\{\text{Ni}(\text{NO})\}^{10}$ species **2**, which displays one of the lowest recorded ν_{NO} values and shares similar structural parameters with MNIC **IIc**. Compound **2** is the first example of an anionic complex containing a $\{\text{Ni}(\text{NO})\}^{10}$ moiety. Although **IIc** is light- and temperature-sensitive and readily converts to a DNIC, **2** is stable, and our efforts to prepare the corresponding nickel dinitrosyl complex have been unsuccessful. The similarity in reactivity of Ph_3CSNO and NO(g) indicates that Ph_3CSNO functions as an NO donor under these reaction conditions. In contrast, addition of NOBF_4 to **1** produced a dimetallic $\{\text{Ni}(\text{NO})\}^{10}$ species that exhibited ^1H NMR and IR spectra different from those of **2**. The resulting thiolate-bridged dimer **3** suggests a possible intermediate in the conversion of one $[\text{2Fe-2S}]$ cluster into two DNICs that has not yet been observed. Complex **3** was also prepared by addition of Me_3OBF_4 to **2**, demonstrating the ability of these two $\{\text{Ni}(\text{NO})\}^{10}$ species to interconvert by simple ligand dissociation or association reactions.

The $\{\text{Co}(\text{NO})_2\}^{10}$ complex **5** can be obtained by reaction of **4** with Ph_3CSNO , NO(g), or NOBF_4 and displays the lowest recorded ν_{NO} values for any dinitrosylcobalt complex with this

(83) Praneeth, V. K. K.; Neese, F.; Lehnert, N. *Inorg. Chem.* **2005**, *44*, 2570–2572.

electron count. Furthermore, **5** is the first example of an anionic complex containing a $\{\text{Co}(\text{NO})_2\}^{10}$ moiety. Attempts to isolate or observe a cobalt mononitrosyl were unsuccessful, presumably due to rapid disproportionation into a cobalt(I) dinitrosyl and a cobalt(III) species. Reaction of **5** with Me_3OBF_4 afforded a trinuclear analogue of RRE **6** composed of three $\{\text{Co}(\text{NO})_2\}^{10}$ units. The existence of this complex suggests a pathway by which RRE might be converted into RBS. RRE might be in equilibrium among various $[\text{Fe}(\text{NO})_2(\mu\text{-SPh})_n]$ species, where the predominant form has $n = 2$, followed by $n = 3$, etc. The trimeric form of RRE could react with one molecule of MNIC to produce RBS and three molecules of thioether. Such chemistry may seem improbable, but iron persulfide complexes can be prepared by insertion of a thiolate into an iron–sulfur bond,⁸⁴ and sulfur can be extruded from iron persulfide complexes.^{85,86} Conversion of RRE into RBS could occur by insertion of a thiolate into an iron–sulfur bond followed by alkyl or aryl transfer within the coordinated disulfide and dissociation of the resultant thioether.

The exploration of the nitric oxide reactivity of homoleptic nickel(II) and cobalt(II) thiolate complexes has yielded interesting coordination compounds and suggests undiscovered reactiv-

ity for the analogous iron(II) complexes. Syntheses of alkyl variants of **2**, **3**, **5**, and **6** will be interesting to pursue for comparison, as will iron analogues of **3**, together with attempts to convert RRE-type complexes to RBS.

Acknowledgment. This work was supported by NSF Grant CHE-0611944. The MIT DCIF NMR spectrometer used was funded through NIH Grant 1S10RR113886-01. A.G.T. is grateful for an NSF predoctoral fellowship, and S.D. is the recipient of an Anna Fuller Fellowship in Molecular Oncology. We thank Dr. Z. Tonzetich for a gift of Ph_3CSNO , experimental assistance, and helpful discussions. We also appreciate helpful comments from Prof. W. D. Jones.

Supporting Information Available: ^1H NMR spectra of **2**, **3**, and an equimolar mixture of the two; X-ray crystallographic data, including tables, ORTEP diagrams, and CIF files, for **2**, **3**, **5**, and **6**. This material is available free of charge via the Internet at <http://pubs.acs.org>.

JA803992Y

(84) Wu, X.; Bose, K. S.; Sinn, E.; Averill, B. A. *Organometallics* **1989**, *8*, 251–253.

(85) Schweitzer, D.; Shearer, J.; Rittenberg, D. K.; Shoner, S. C.; Ellison, J. J.; Loloee, R.; Lovell, S.; Barnhart, D.; Kovacs, J. A. *Inorg. Chem.* **2002**, *41*, 3128–3136.

(86) Coucouvanis, D.; Lippard, S. J. *J. Am. Chem. Soc.* **1968**, *90*, 3281–3282.